Article no. 10

THE CIVIL ENGINEERING JOURNAL 1-2018

SEISMIC RESPONSE ANALYSIS OF LONG-SPAN CABLE-STAYED BRIDGE WITH NONLINEAR VISCOUS DAMPERS UNDER DIFFERENT PERIODIC SEISMIC WAVES

Chen Baiben, Feng Zhongren and You Huimin

Wuhan University of Technology, School of Civil Engineering and Architecture, Wuhan 430070, China; cbb0505@163.com, fengz515@163.com, youhuimin@whut.edu.cn

ABSTRACT

In order to study the effect of nonlinear viscous dampers on the seismic response of long-span cable-stayed bridge under different periodic seismic waves, as Erdong Yangtze River Bridge which main span is 926 meters in Hubei province of China for the research object, nonlinear viscous dampers are simulated by Maxwell model, and four viscous dampers are set at the joint of main tower and beam. The displacement and internal force responses of cable-stayed bridge with different velocity index and damping coefficient of nonlinear viscous dampers are analysed and discussed, in the situation of that long period and ordinary period seismic waves are input as earthquake motions. Analysis results show that: the displacement and internal force responses of long-span cable-stayed bridge under long period seismic wave are more negative; the displacements of key nodes of bridge can be reduced effectively by nonlinear viscous dampers; the internal force responses of bridge would be influenced greatly by the combination of different parameters of viscous dampers; the growth of shear and bending moment at the bottom of the tower can be controlled in an acceptable range by the reasonable parameter combination; the ideal parameter combination is that velocity index of viscous damper is 0.6 and the damping coefficient is 7000 $N.(s/m)^{\alpha}$ for this cable-stayed bridge under long-period seismic wave.

KEYWORDS

Long-span cable-stayed bridge, Nonlinear viscous dampers, Periodic characteristics of seismic waves, Maxwell model, Velocity index, Damping coefficient

INTRODUCTION

Since twenty-first century, the Earth has entered a period of frequent earthquakes. Especially in the past 10 years, earthquakes with high magnitude and strong intensity have occurred frequently, which endanger the safety of human life and property seriously, and affect social stability and economic development. Since 2014, more than 57 earthquakes which magnitude over 7 have occurred all of the world, including a magnitude 8.1 earthquake occurred in Nepal in April 2015, a magnitude 8.2 earthquake occurred in Chile in September 2015 and a magnitude 8.0 earthquake occurred in New Zealand in November 2011. Strong earthquake will not only cause huge casualties, but will also lead to destruction of transportation infrastructure, and will affect the rescue and disaster relief operations. Bridge as the joint of transport line, the consequences will be unbearable if it has been destroyed, not only delay the rescue work, but also unable to quickly transfer trapped people who may suffer damage of secondary disasters caused by the earthquake [1]. In the view of this, it is significant to improve the seismic performance of bridges and reduce

the damage under earthquake with different magnitude.

The long-span cable-stayed bridge, as the key of the traffic line, needs to be paid more attention to its aseismatic performance and disaster prevention work. At present, with the deepening of the concept of energy dissipation and earthquake reducing, energy dissipation device applied in the large bridge structure, especially the seismic isolation bearings and viscous dampers, provide new ideas and methods to the traditional concept of seismic ductility design [2]. The research on the longitudinal seismic theory of cable-stayed bridge and related engineering practice shows that the longitudinal displacements of beam and main tower top can be reduced effectively and the stress state of structure would be improved under ordinary period seismic wave when placed longitudinal viscous dampers [3-5].

The damping effect of nonlinear viscous damper on bridge is related to its main parameters closely, reasonable parameters not only can improve seismic response reduction of the long-span cable-stayed bridge effectively, but also can achieve the optimum in economy, technology and construction [6]. At present, many scholars have carried out relevant research on parameter optimization of viscous dampers. The experimental study on the stiffness of the damper was carried out by Jennifer Anne Fournier [7]. The study discussed the influence of the damping stiffness and the support stiffness of the damper on the seismic reduction effect. The relevant research about damping parameters which considered pile-soil interaction was studied by Jin Zhu [8] and given the optimum parameters. The fitting equation of optimal damping parameters have been given based the least squares regression analysis method by Shengpin Wu [9]. The function expression for the viscous damping parameters of the seismic response of the structure have been given by Bo Wang [10] according to the response surface method based on the pseudo excitation method. Wenxue Zhang [11] analysed the influence of the relative height of the bridge deck and viscous damper on the damping effect of the cable-stayed bridge. However, these studies mainly focus on the seismic response under ordinary period ground motion, without considering the long period ground motion. The relative research showed that the adverse effect of long period ground motion is more obvious due to the large flexibility of long-span structure and longer natural vibration period [12-13]. Because the spectral characteristics of long period ground motions are different from those of ordinary ground motions, the reasonable parameters will also change.

Based on the time domain and frequency domain characteristics of ground motion with different periods, as Chinese Erdong Yangtze River Bridge with the main span of 926 meters for engineering background, the optimum parameters of nonlinear viscous dampers are analysed under the action of earthquake with different period characteristics, which can provide reference for seismic design of long-span cable-stayed bridges. By using the finite element software ANSYS to establish three-dimensional finite element model of the whole bridge, and through the Maxwell model to simulate the nonlinear viscous dampers, a damping and energy dissipation scheme with four nonlinear viscous dampers installed at the joint of tower and beam is presented. Through the comparison and analysis of the displacement and internal force responses of bridge, the influence trend of different parameters of viscous dampers is determined, and the optimal parameter combination of viscous dampers will be obtained.

NONLINEAR VISCOUS DAMPER

Mechanical characteristics of nonlinear viscous damper

According to the relationship between damping force and relative velocity, viscous damper can be divided into linear damper and nonlinear damper [14]. The general expression of damping force is as follows:

$$F = C\,\mathrm{sgn}(\dot{x})|\dot{x}|^{\alpha} \tag{1}$$

In the formula: $\dot{x}$ is the relative velocity of the damper, C is the damping coefficient, $\mathrm{sgn}()$ is the coincidence function, α is the velocity index. When $\alpha = 1$, a linear damper was used; when $\alpha < 1$, the nonlinear viscous damper was used; when $\alpha < 1$, the superlinear viscous damper was considered.

The nonlinear viscous damper and linear viscous damper exhibit different mechanical characteristics when the velocity index is different. In the smaller velocity cases, the force value of nonlinear viscous damper was bigger than that of the linear viscous damper. As the velocity increases, the increasing amplitude of force value of nonlinear viscous damper becomes smaller, but that of linear viscous damper increases continuously in a fixed proportion; when the velocity exceeds a certain value, the force value of the viscous damper increases rapidly with the increase of the velocity [15]. This can improve the seismic capacity of the structure to a certain extent, but it also may be possible to cause the failure of the viscous damper, because of that the strength of the connector is not enough. The nonlinear viscous damper force value tends to be stable when the velocity reaches a certain value. Figure 1 is the damping force value of the viscous damper varying with the change of velocity.

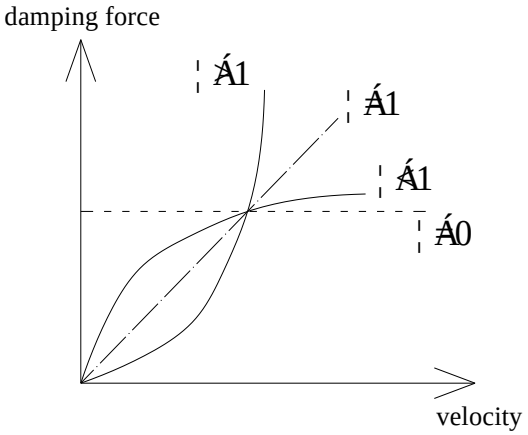

Fig. 1 - Characteristic curve of viscous damper

Dynamic analysis model of damper

Simulation model of viscous damper is based on Maxwell model. The damper model consists of pure damping element and spring element connected in series [16]. The Maxwell model is shown in Figure 2.

Fig. 2 - Maxwell model

The displacement of the damping element is set to $u_1(t)$ and the spring element is set to $u_2(t)$. According to the force state of the model, the formula can be made up of the following:

$$u_1(t) + u_2(t) = u(t) \tag{2}$$

$$F(t) = C_0\dot{u}_1(t) = Ku_2(t) \tag{3}$$

In the formula: $F(t)$ is the damping resistance, C_0 is the linear damping constant at zero frequency, and K is stiffness coefficient in wireless large frequency domain.

It can be obtained by formula (2) and (3):

$$\dot{F}(t) + \lambda F(t) = C_0 \ddot{u}_1(t) \tag{4}$$

$$\dot{F}(t) = f(F, u, \dot{u}) = -\frac{1}{\lambda} F(t) + \frac{C_0}{\lambda} \ddot{u}_1(t) \tag{5}$$

Among the formula: λ is the time factor, $\lambda = C_0 / K$ 。

Based on the structural characteristics of bridge with dampers, the ground motion equation can be expressed as:

$$M_s \ddot{x}_s(t) + C_s \dot{x}_s(t) + K_s x_s(t) + \sum_{d=1}^{n} r_d P_d(t) = -M_s I \ddot{X}_g(t) \tag{6}$$

In the formula: M_s, C_s, K_s indicate quality, internal damping and stiffness matrix respectively. I is the influence coefficient matrix of ground motion. $\ddot{X}_g(t)$ is the acceleration time-histories. $x_s(t)$ is the structural dynamic displacement matrix. $P_d(t)$ is the damping force of damper. r_d is the damping influence matrix.

Engineering background and finite element model

Engineering background

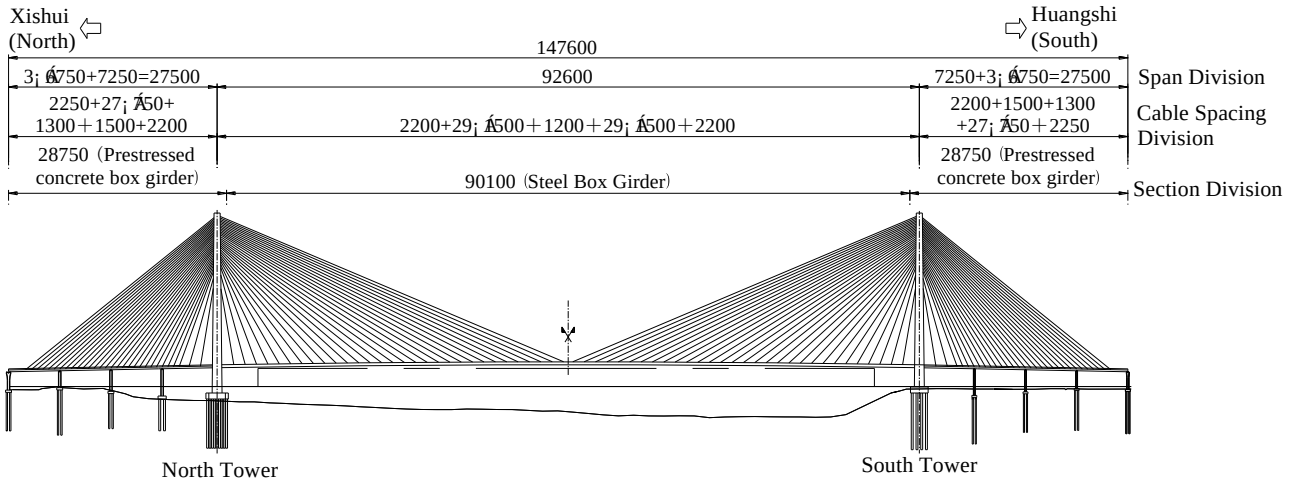

Fig. 3 - General view of Erdong Yangtze River Bridge (unit: cm)

Erdong Yangtze River Bridge is located between Huangshi and Erzhou in Hubei province of China. The bridge is a half floating cable-stayed bridge which has nine spans, two towers and composite beam. The arrangement of bridge spans is 3×67.5m +72.5m +926m +72.5m +3×67.5m =1476m. Three auxiliary piers and a transitional pier are set in side span, and the full width of bridge deck is 36m. The separated steel box girder is used in the middle span of bridge, and the separated concrete box girder is used in the side span. The interface of steel and concrete is set at middle span which has 12.5m away from the centre line of the tower. The whole bridge has 120 pairs of cables. General view of Erdong Yangtze River Bridge is shown in Figure 3.

Finite element model

Three-dimensional model of full bridge is established by finite element software ANSYS. In order to take into account local vibration of cables, multiple-element cable system model is used to simulate cables, and the unit of cable is divided according to the length. The main beam is simulated like fishbone. The main beam, main towers and pier column are established by beam188 element, the stay cables are established by link10 element, and the fishbone of beam is established by beam4 element. The viscous dampers are simulated by combin37 element. This element is a nonlinear spring element, and the complex spring damping model can be simulated by parameter setting. The bottom of the stay-cable is connected with the end of the fishbone of the beam, and the top is coupled with the main tower unit. The cable force of the completed bridge is input, and the geometric stiffness of the dead load is considered in the structural model. The finite element model is shown in Figure 4.

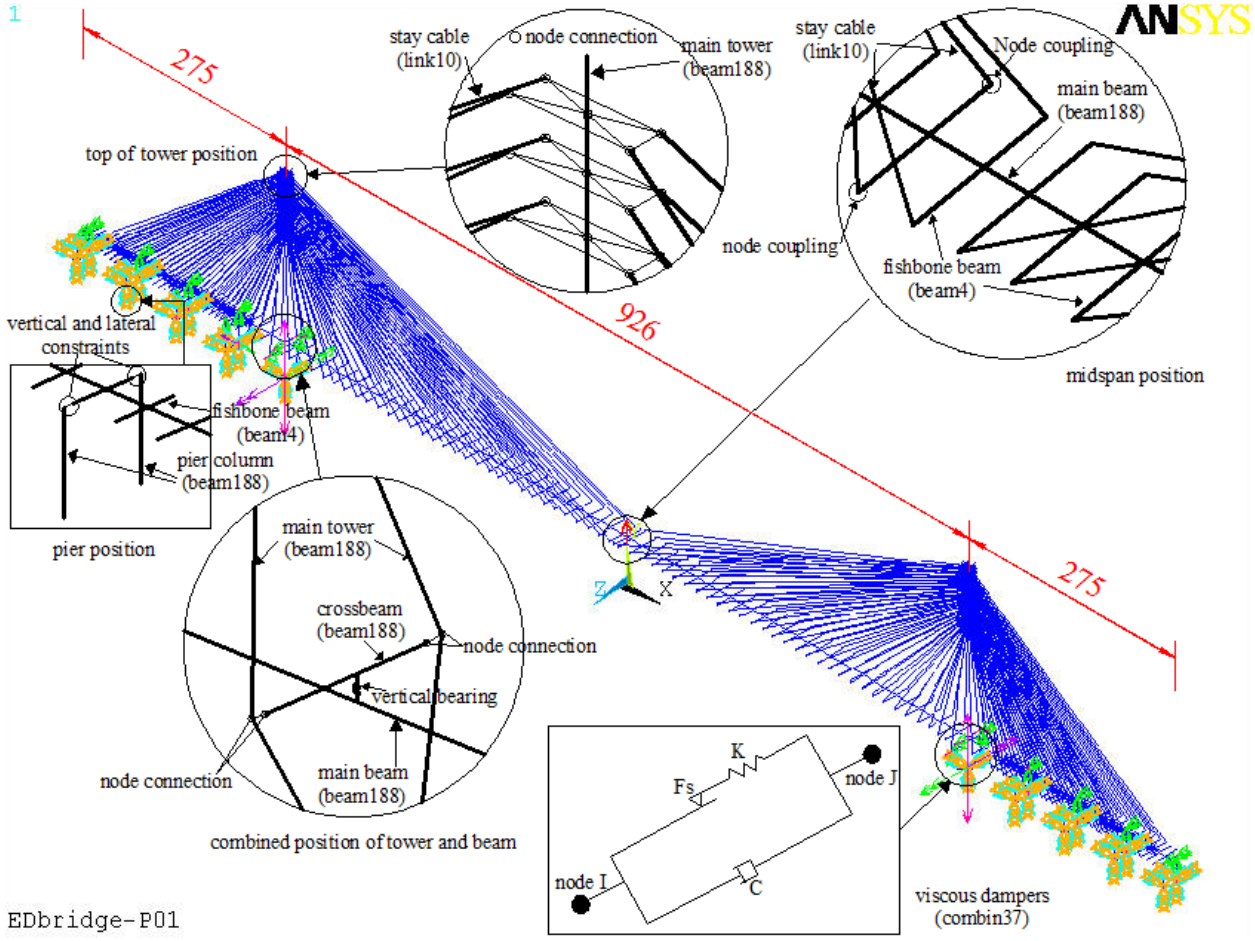

Fig. 4 - Finite element model of bridge (unit: m)

Geometric nonlinear behaviour

The geometric nonlinear behaviour of long-span cable-stayed bridge is very significant, and it should be taken into account in the analysis. The geometric nonlinear factors of long-span cable-stayed bridges include three aspects: (1) the beam column effect (P - delta effect) resulting from the interaction of axial force and bending moment in main girder and main tower; (2) geometric change caused by large displacement; (3) the sag effect of stay cables.

The ANSYS system is used to consider the geometric nonlinear behaviour of long-span cable-stayed bridges in this case. By using the command "NLGEOM, ON" to activate the large displacement effect of the structure, the geometric change caused by the large displacement effect will be automatically counted by the model. At the same time, the program opens the stress stiffening switch with the command "SSTIF, ON" for calculating the initial stress stiffness matrix, which contains the effect of P - delta effect. For the influence of the sag effect of stay cables, the equivalent elastic modulus method or the segmental link element method are adopted in the traditional simulation methods. The equivalent elastic modulus method is used to modify the elastic model of cables by using the Ernst formula. This method can take into account the nonlinear behaviour of cables, but the accuracy is low. In this study, the sag effect of cables is simulated by the segmental link element method. Combined with the computational accuracy and efficiency of the model, according to the length of the cable, the length of each cable is evenly divided with a maximum length of 50m, and the number of segments of each cable is bounded between 3~10 sections.

Dynamic characteristic analysis

The vibration characteristics of the structure are analysed by using Block Lanczos method. The dynamic characteristics of the whole bridge can be obtained by comparing the model with and without damper, as shown in Table 1. The first order frequency of the whole bridge is smaller, and the natural vibration period is about 11.1s, which reflects that this bridge is a long-period structure. The longitudinal vibration is the worst condition. When the viscous dampers are applied, the natural frequency of the bridge and the stiffness of the structure increases slightly, but the amplitude is limited. It shows that the viscous dampers do not completely change the mass and stiffness distribution of the bridge, and have little influence on the structural force system under static load. However, the function of viscous dampers occurs under dynamic load basically, and the viscous damping force acts as a function of energy dissipation with the change of the external load.

Tab. 1 - Natural vibration frequency of the bridge (Hz)

Order	Model without damper	Model with damper	Vibration characteristics
1	0.0965	0.0973	Longitudinal floating of main beam
2	0.1667	0.1728	First order symmetrical lateral bending of main beam
3	0.2234	0.2316	First order symmetrical vertical bending of main beam
4	0.2766	0.2855	First order antisymmetric vertical bending of the main beam
5	0.3799	0.3921	Second order symmetrical vertical bending of main beam
6	0.4500	0.4637	Second order antisymmetric vertical bending of main beam
7	0.4556	0.4694	First order antisymmetric lateral bending of the main beam
8	0.5250	0.5402	Third order symmetrical vertical bending of main beam
9	0.5782	0.5785	Lateral bending of towers
10	0.6109	0.6167	Third order antisymmetric vertical bending of main beam

Ground motion characteristics

(1) Time domain characteristics

Long period seismic waves have the characteristics of long duration and rich low-frequency components. In order to study the characteristics of long period ground motions, three long period seismic waves are compared with three ordinary seismic waves. Long period seismic waves are the TCU026 (NS) wave and TCU136(EW) wave recorded by the bedrock site during the Chichi earthquake in Taiwan in 1999, and the CBGS (N89W) wave recorded by Christchurch Botanical Gardens station in Darfield earthquake occurred in New Zealand Canterbury in 2010. The selected

ordinary seismic waves are EI Centro (NS) wave, Taft (N21E) wave and San Fernando wave. Comparison of time domain characteristics is shown in Table 2. Acceleration time histories charts of six seismic waves are shown in Figure 5. By time domain characteristics analysis, it can be obtained that long period seismic waves have more rich long period elements and longer duration compared with the ordinary seismic waves, but the peak acceleration is generally small. The maximum peak acceleration always occurs at a later time.

Tab. 2: Characteristics comparison of six seismic waves

Seismic wave*	Year	Magnitude	Peak acceleration (gal)	Recording time (s)
TCU026(NS)	1999	7.6	73.4	90
TCU136(EW)	1999	7.6	117.9	90
CBGS(N89W)	2010	7.0	139.8	150
EI Centro(NS)	1940	6.4	341.7	53.76
Taft(N21E)	1952	7.7	152.7	54.38
San Fernando	1971	6.5	207.9	28

* The seismic waves from the seismic database of Pacific Earthquake Engineering Research Center. The unit 'gal' is cm/s^2.

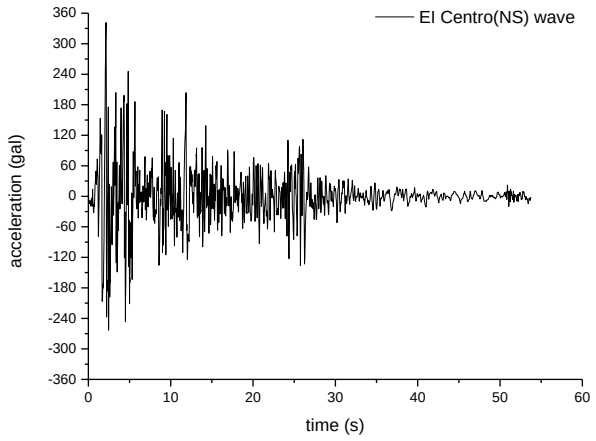

(a) Time domain characteristic of EI Centro(NS) wave

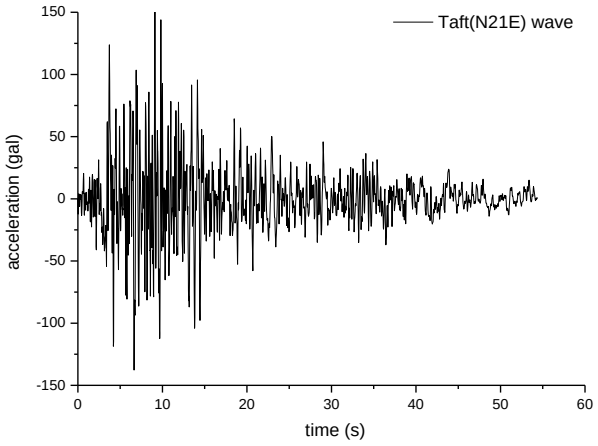

(b) Time domain characteristic of Taft(N21E) wave

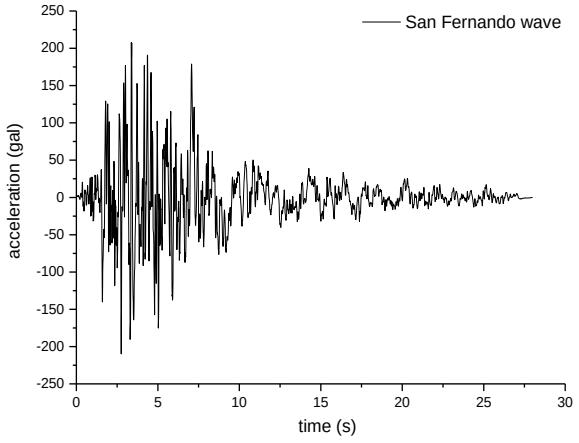

(c) Time domain characteristic of San Fernando wave

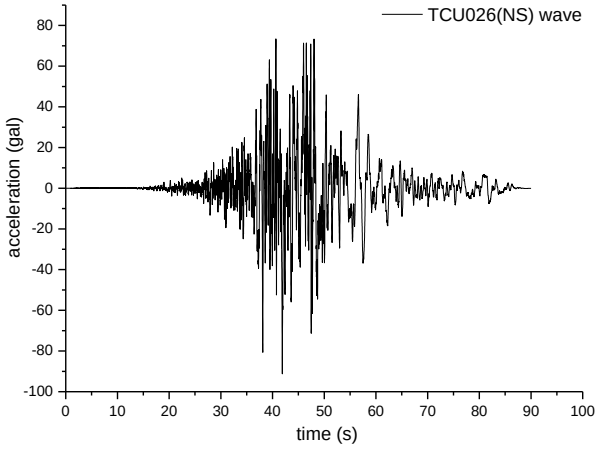

(d) Time domain characteristic of TCU026(NS) wave

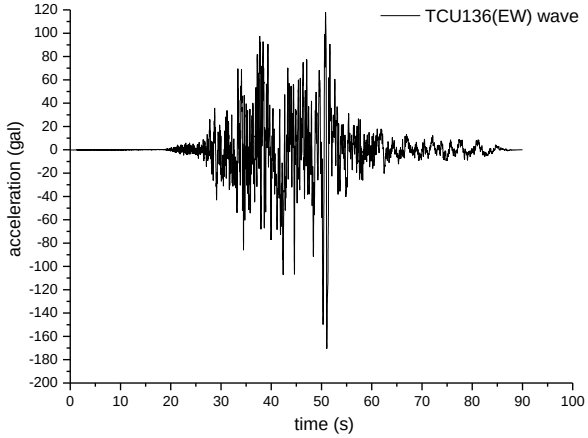

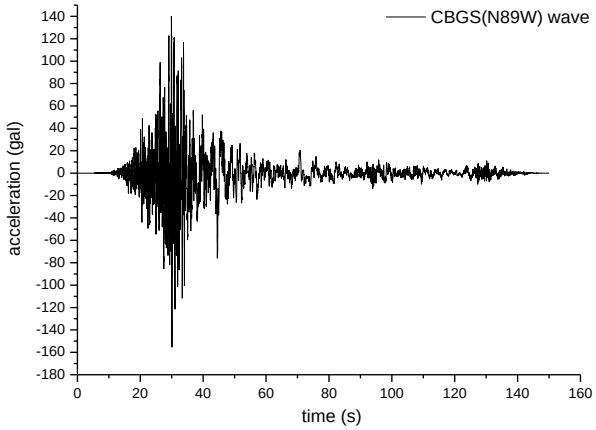

(e) Time domain characteristic of TCU136(EW) wave (f) Time domain characteristic of CBGS(N89W) wave

Fig. 5 - Acceleration time curve of seismic waves

(2) Frequency domain characteristics

Compared with ordinary period seismic waves, long period seismic waves also have their unique features in the frequency domain. Fourier spectrums can show the frequency characteristics of seismic waves. The Fast Fourier Transform (FFT) of six seismic waves are carried out by using the mathematical software MATLAB, and the Fourier amplitude spectrums of seismic waves are compared. The Fourier amplitude spectrums of the six seismic waves are shown in Figure 6. From this figure, The El Centro(NS) wave is mainly composed of 1 ~ 4Hz, the Taft(N21E) wave is 1～5Hz, and San Fernando wave is 0.5～6Hz, which of them have high frequency components. But contrary, the frequency of TCU026 (NS) wave mainly concentrated between 0.1 and 1.7Hz, TCU136(EW) is 0.1～1Hz, and CBGS(N89W) is 0.2～2Hz, the main frequencies of above waves are concentrated in the low frequency range.

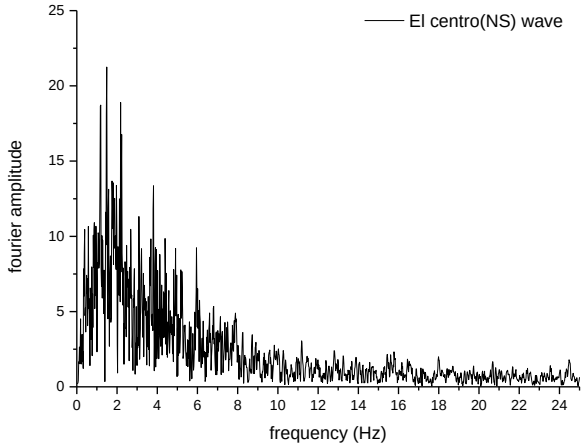

(a) Frequency domain characteristic of El Centro(NS) wave

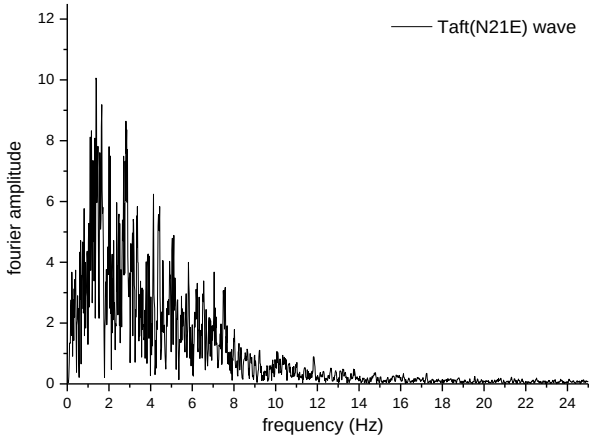

(b) Frequency domain characteristic of Taft(N21E) wave

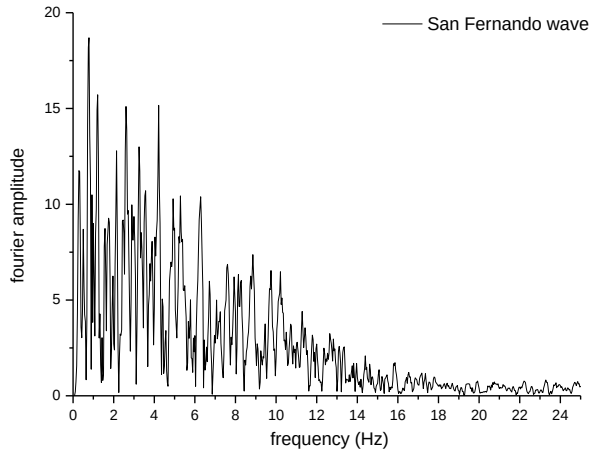

(c) Frequency domain characteristic of San Fernando wave

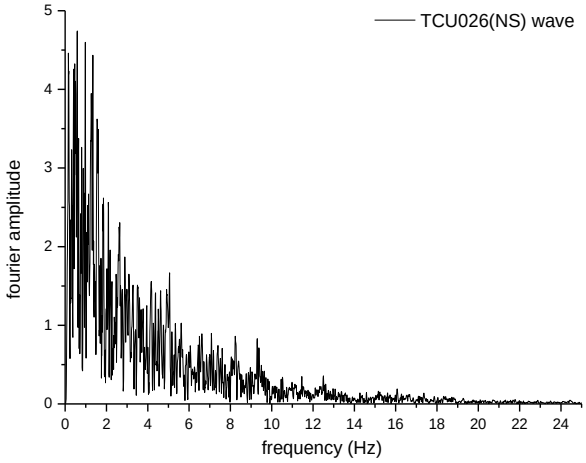

(d) Frequency domain characteristic of TCU026(NS) wave

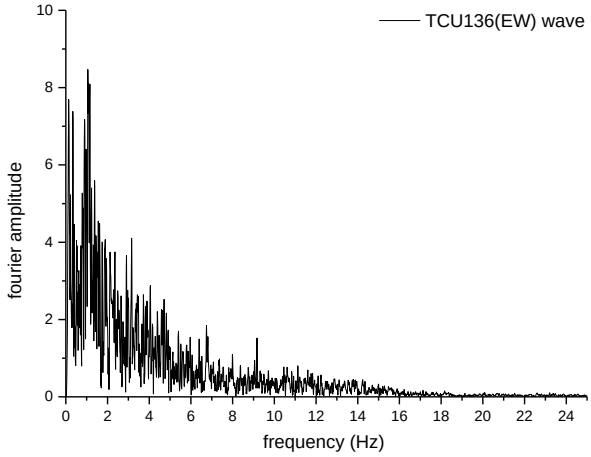

(e) Frequency domain characteristic of TCU136(EW) wave

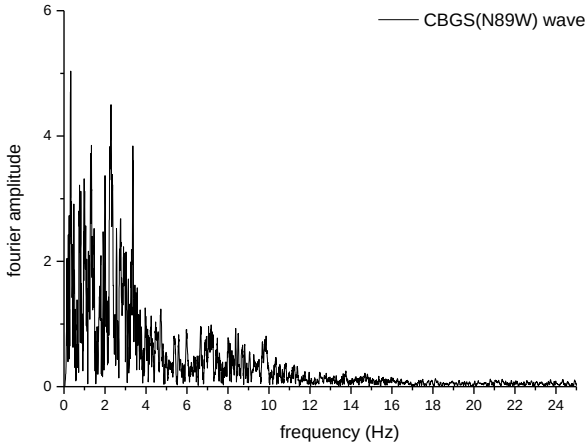

(f) Frequency domain characteristic of CBGS(N89W) wave

Fig. 6 - Fourier amplitude spectrums of seismic waves

(3) Comparison of acceleration response spectrum

The acceleration response spectrum can reflect the influence of seismic wave within the time range on the structure. In order to show the difference between long period seismic wave and ordinary period seismic wave, the standard acceleration response spectrums of them are plotted when the damping ratio is 5%, as shown in Figure 7. It can be seen from the diagrams that the amplification coefficient β of long period seismic wave in the long period is obviously larger than that of the ordinary period seismic wave. The amplification effect of ordinary seismic wave on the structure is mainly concentrated in the range of 0 ~ 2.5s, and the effect of long period seismic wave is from 0 to 9s, which have very wide periodic domains. From that, the long-period component of long period seismic wave has a negligible effect on the seismic response of the structure, which will have a significant effect on the vibration of the structure with longer natural vibration period.

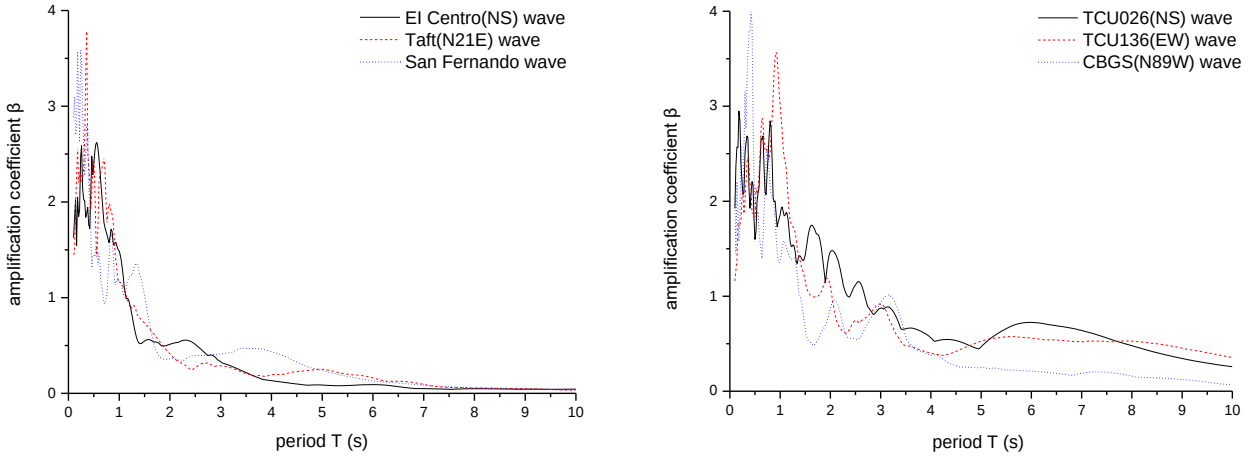

(a) Acceleration response spectrum of ordinary period seismic waves

(b) Acceleration response spectrum of long-period seismic waves

Fig. 7 - Standard acceleration response spectrums of seismic waves

(4) Seismic wave input

In order to compare the effect of long period seismic wave and ordinary periodic seismic wave, considering the seismic response of bridge with viscous dampers, the EI Centro (NS) wave and the TCU026 (NS) wave are chosen as the representations for comparative analysis. According to the bridge site safety assessment report, the acceleration peak values of the selected seismic wave are adjusted to 0.126g. The ground motion along the longitudinal direction of the bridge is taken into account without considering the influence of lateral and vertical ground motion.

Setting scheme of viscous dampers

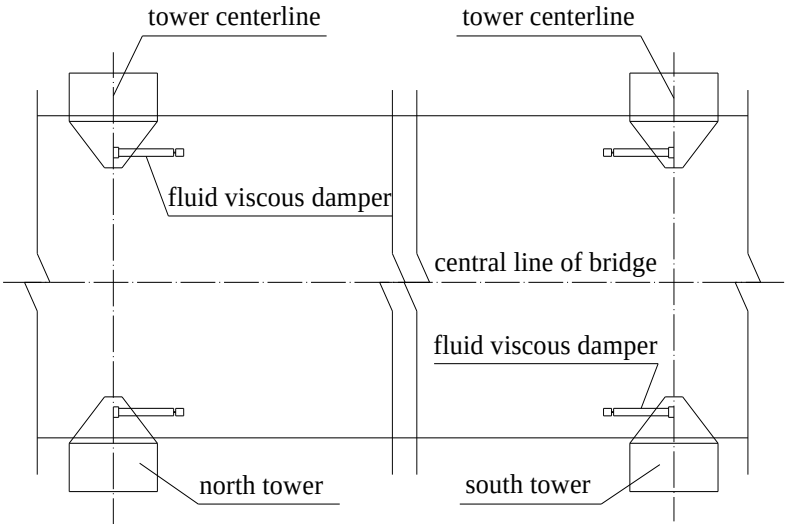

Fig. 8 - Setting position of nonlinear viscous dampers

The installation of viscous dampers for long-span cable-stayed bridge is usually located at the connection position between the main tower and beam, or the location of the auxiliary piers. However, because of the small space and the complex cable system in the auxiliary pier, it is

difficult to add viscous dampers. A viscous damper scheme is adopted at the joint of the tower and the beam for this study, considering the force state and the actual state of the whole bridge. Four viscous dampers along the bridge were set, two of which are at the joint of main beam and north tower, and others are set at the connection position between the main beam and south tower. As shown in Figure 8.

Parameter analysis of viscous dampers

By analysing the mechanical characteristics of viscous dampers, it is found that the damping coefficient C and velocity index α will affect the damping force of the damper, thus changing the seismic response of the structure. By analyzing the changes of damping coefficient C and velocity index α of viscous damper, the trend of structural response can be obtained, so as to determine the reasonable parameters setting of nonlinear viscous dampers under the action of earthquake with different periodic characteristics. According to the conventional range of damping coefficient and velocity index of the viscous dampers, the damping coefficient C =2000, 3000, 5000, 7000, 10000 *N.(s/m)*$^{\alpha}$ and the velocity index α =0.2, 0.4, 0.6, 0.8, 1 were selected to be combined. A total of 25 combining cases are used for parameter analysis.

Displacement analysis

(1) Displacement analysis under ordinary period ground motion

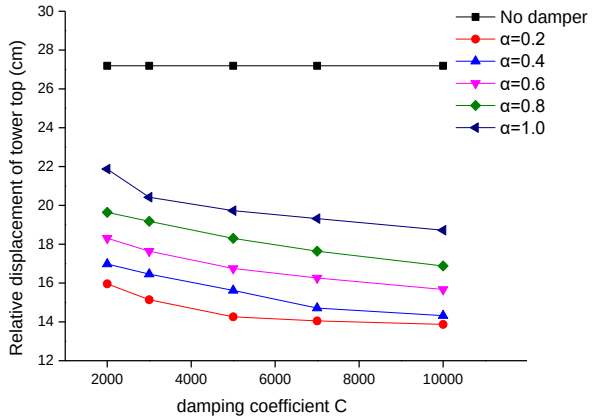

Fig. 9 - Comparison of relative displacements at the top of tower under ordinary period ground motion

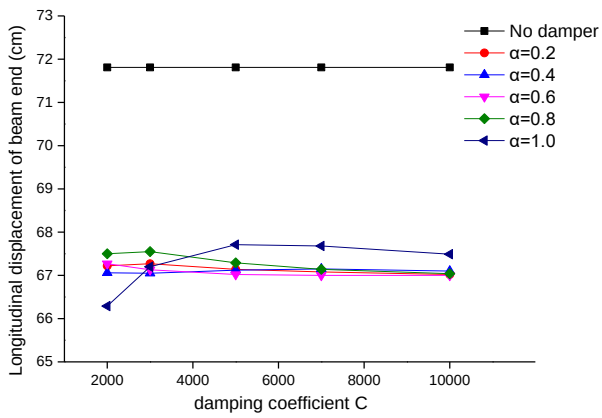

Fig. 10 - Comparison of longitudinal displacements of beam end under ordinary period ground motion

Taking the longitudinal relative displacement of the beam and north tower as the research object, setting viscous dampers has certain effect on reducing longitudinal relative displacement under the action of normal periodic ground motion. The relative displacement is reduced by 19.6% ~ 49% with different combination parameters. The relative displacement of tower top varies regularly with the change of damper coefficient C and velocity index α. When the velocity index increases, the displacement at the top of tower increases gradually; when the damping coefficient increases, the displacement decreases gradually; the relatively superior parameter combination is that: the velocity index of the nonlinear viscous damper is 0.2~0.8, and the damping coefficient is between 5000~10000.

Based on the displacement analysis at the north beam end, as Figure 10 shown, viscous dampers also have good effects on reducing the longitudinal displacement. When velocity index

α =1.0, the longitudinal displacement increases firstly and then decreases with the increase of the damping coefficient; when velocity index α = 0.2~0.8, the displacement decreases with the increase of the damping coefficient. The degree of the change is very small, and the effect can be negligible.

(2) Displacement analysis under long period ground motion

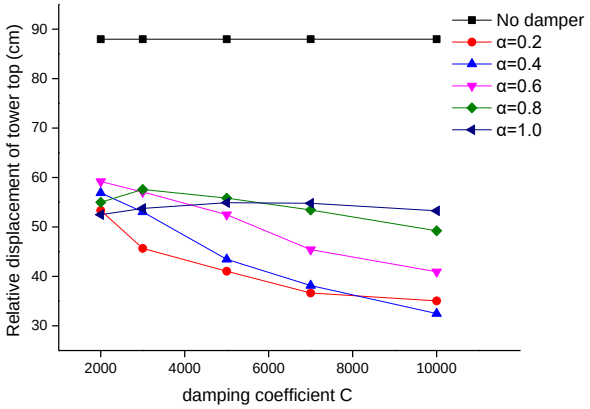

Fig. 11 - Comparison of relative displacements at the top of tower under long-period ground motion

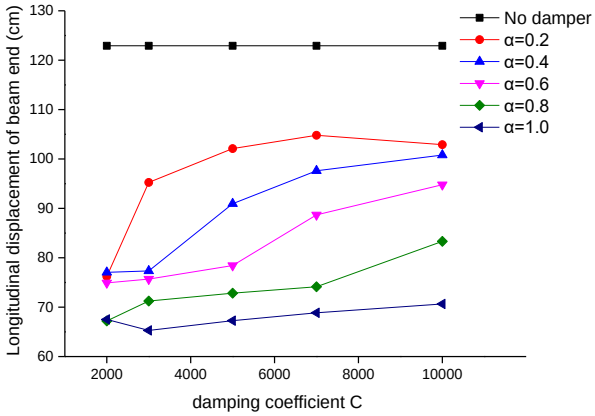

Fig. 12 - Comparison of longitudinal displacements of beam end under long-period ground motion

From Figure 11, the relative displacement of the tower top is reduced obviously after the viscous dampers are set. When the velocity index α =0.2, 0.4 and 0.6, the longitudinal relative displacement of the tower top shows a decreasing trend with the increase of damping coefficient; when the velocity index α =0.8 and 1, the longitudinal displacement increases firstly and then decreases with the increase of damping coefficient. Especially when α =0.4, the best result are got. In this situation, the longitudinal displacement has reduced to only 39.8% when C =10000. From the aspect of reducing the longitudinal relative displacement at the top of tower, in order to reduce the influence of long period ground motion on structure, the best parameter combination is like that: velocity index α is 0.2~0.6, and damping coefficient C is 5000~10000.

It can be concluded from the Figure 12 that the longitudinal displacement of the beam end is obviously reduced after the viscous dampers set, and the difference is obvious with the change of the velocity index and damping coefficient. The displacement of the beam end decreases gradually with the increase of the velocity index. When the velocity index α =1.0, the maximum reduction is 46.9%. The effect of damping coefficient C change on displacement of beam end is related to velocity index. When the velocity index α =0.2, the displacement at the beam end increases firstly and then decreases with the increase of the damping coefficient C, but the amplitude shows an increase trend, and when the damping coefficient C varies from 2000 to 3000, the displacement increases rapidly; when the velocity index α =0.4~1, the displacement of the beam end increases with the increase of the damping coefficient, and the smaller the velocity index is, the larger the amplitude is. In order to reduce the displacement of the beam end after viscous dampers setting, the velocity index of nonlinear viscous damper is 0.6~1 and the damping coefficient is 2000~7000 are the best.

(3) Comparative analysis of displacements

In order to compare the maximum relative displacement at the top of the tower and the maximum displacement at the beam end under the action of ordinary period seismic wave and long period seismic wave, the damping effects of viscous dampers with different parameters are analysed. As the displacement response of the structure without viscous dampers for 1, the displacement response data with viscous dampers are normalized. For instance, assuming structural displacement response without viscous dampers for x_1, displacement response with viscous dampers for x_2, normalized value is $v = x_2 / x_1$. The comparison is shown in Table 3.

Tab. 3 - Displacement contrast analysis of different period seismic waves

damping Coefficient*		No damper		2000		3000	
		ordinary	long	ordinary	long	ordinary	long
velocity index		absolute value		normalized value		normalized value	
displacements at the top of tower (cm)	0.2	27.19	87.97	0.587	0.606	0.557	0.519
	0.4	27.19	87.97	0.624	0.647	0.605	0.603
	0.6	27.19	87.97	0.673	0.673	0.649	0.649
	0.8	27.19	87.97	0.722	0.625	0.705	0.655
	1	27.19	87.97	0.804	0.596	0.751	0.611
displacements of beam end (cm)	0.2	71.81	122.92	0.936	0.620	0.937	0.775
	0.4	71.81	122.92	0.934	0.627	0.934	0.629
	0.6	71.81	122.92	0.937	0.610	0.935	0.616
	0.8	71.81	122.92	0.940	0.547	0.941	0.580
	1	71.81	122.92	0.923	0.549	0.936	0.531
damping coefficient		5000		7000		10000	
		ordinary	long	ordinary	ordinary	long	ordinary
velocity index		normalized value		normalized value		normalized value	
displacements at the top of tower	0.2	0.524	0.467	0.517	0.417	0.510	0.398
	0.4	0.574	0.494	0.541	0.434	0.527	0.369
	0.6	0.616	0.596	0.598	0.516	0.576	0.465
	0.8	0.673	0.635	0.649	0.607	0.621	0.560
	1	0.726	0.624	0.711	0.623	0.688	0.605
displacements of beam end	0.2	0.935	0.831	0.934	0.853	0.933	0.837
	0.4	0.935	0.740	0.935	0.794	0.934	0.820
	0.6	0.933	0.638	0.933	0.721	0.933	0.771
	0.8	0.937	0.592	0.935	0.603	0.934	0.678
	1	0.943	0.547	0.942	0.560	0.940	0.575

* 'ordinary' stands for ordinary period seismic wave, 'long' stands for long-period seismic wave.

It can be seen from the Table 3 that the displacement responses of the structure under the action of long period ground motion are much larger than that under the ordinary ground motion without the viscous damper. This shows that the long period ground motion has more negative impact on the structure. From the displacement response of bridge with viscous dampers, the damping effect of viscous dampers under long period ground motion is more obvious. In contrast, the damping effect of viscous dampers under the ordinary seismic wave is in general level. Especially for the displacement of beam end, the maximum reduction is only 7.7%.

From the above analysis, in the seismic design of reducing the displacements of the main nodes, the seismic response under the action of long period ground motion should be chosen as a key issue to be considered.

Internal force analysis

(1) Internal force analysis under ordinary period ground motion

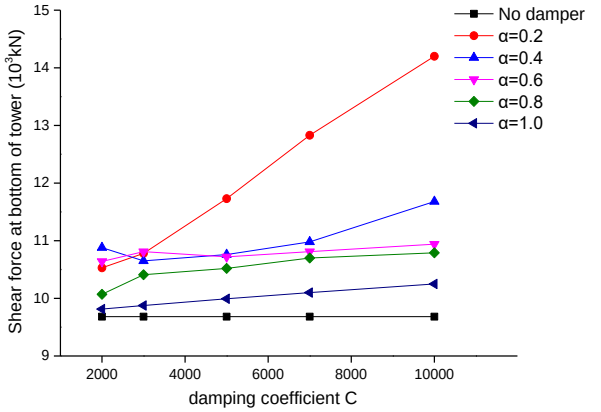

Fig. 13 - Comparison of shear forces at the bottom of tower under ordinary period ground motion

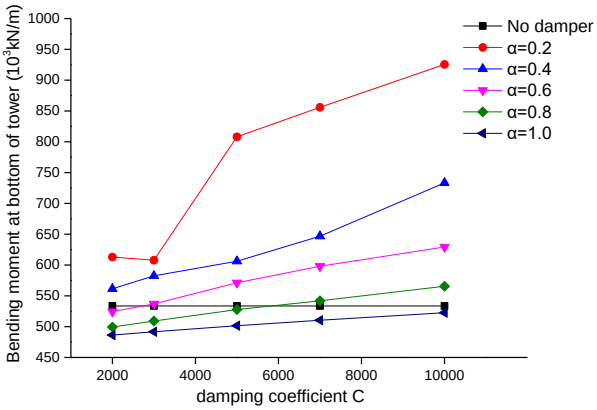

Fig. 14 - Comparison of bending moment at the bottom of tower under ordinary period ground motion

The analysis about shear at the bottom of north tower was done in Figure 13. The different growth trends for the shear force were shown after the viscous dampers are installed under ordinary seismic wave. When the velocity index is 0.2, the shear growing is the fastest and the stress state is the most unfavourable. Especially when the damping coefficient C increases, the shear at the bottom of the tower increases relatively.

Aiming at the bending moment at the bottom of tower, from Figure 14, the effects of different parameters combination on the bending moment are obviously different. In most cases, bending moment will increase after viscous dampers setting, and the bending moment of tower bottom increases more obviously with the increase of the damping coefficient. And yet, bending moment will reduce significantly with the increase of velocity index. When the velocity index α is 1.0, the moment at the bottom of the tower with viscous dampers is less than it without viscous dampers.

(2) Internal force analysis under long period ground motion

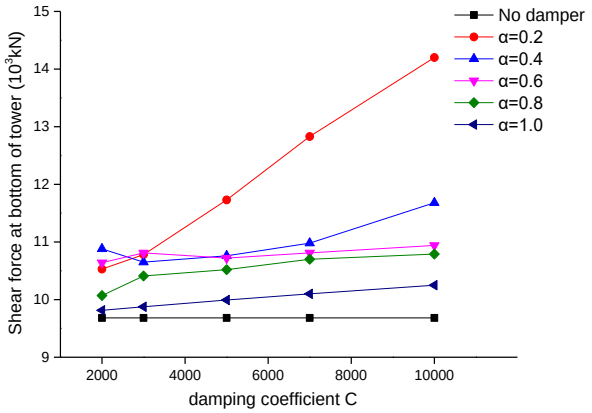

Fig. 15 - Comparison of shear forces at the bottom of tower under long-period ground motion

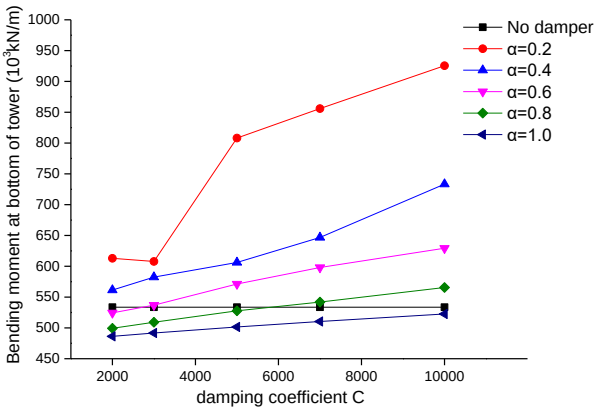

Fig. 16 - Comparison of bending moment at thebottom of tower under long-period ground motion

From the Figure 15, it can be concluded that the shear force at the bottom of the tower have different increasing trends with different parameter combinations of the viscous dampers under the action of long period ground motion. When the velocity index α=0.2, the shear force increases rapidly with the increasing of damping coefficient. The maximum increase rate is 116.7%. It means that the smaller velocity index is not conducive to the shear controlling. Additionally, the shear would be affect by the damping coefficient changing in different velocity index range. When the velocity index is 0.4~0.8, the shear increases firstly and then decreases. The disadvantageous situations are as followed: (1) α=0.4, C=3000; (2) α=0.6, C=5000; (3) α=0.8, C=7000. When the velocity index is 1.0, the shear force is smaller than other situation, and has linear growth state with the increase of damping coefficient. Under the action of long period ground motion, setting viscous dampers will have unfavourable effect to the shear force response. But compared with the reducing of displacement, the shear increasing amplitude by the reasonable parameter combinations is unobvious. The parameters should be selected to avoid the great increasing of shear.

The comparison of bending moment of north tower is shown in Figure 16. The setting of viscous dampers will greatly increase the bending moment at the bottom of the tower, and change the stress state of the main tower. But the reasonable parameters of viscous dampers can effectively control the bending moment, and make sure that the bending moment is in a controllable range. Besides, some parameters can reduce the bending moment slightly, and achieve the best state of stress for the whole bridge. From the moment contrast diagram, the unreasonable combinations are like that: (1) α=0.2, C=5000 ~ 10000; (2) α =0.4, C=10000. In the situation of above combinations, the bending moment increases obviously. The most ideal parameter combinations are that: velocity index α=0.2 and damping coefficient C=3000; velocity index α=0.6 and damping coefficient C=7000. With this parameter combination, the bending moment decreases slightly compared with that without the viscous dampers.

(3) Comparative analysis of internal force

Based on the above research, the force analysis data were normalized, and as shown in Table 4.

Tab. 4: Internal force contrast analysis of different period seismic waves

damping coefficient*		No damper		2000		3000	
		ordinary	long	ordinary	long	ordinary	long
velocity index		absolute value		normalized value		normalized value	
shear forces at the bottom of tower (10^3kN)	0.2	9.683	14.96	1.087	1.461	1.113	1.665
	0.4	9.683	14.96	1.124	1.257	1.100	1.469
	0.6	9.683	14.96	1.099	1.174	1.116	1.239
	0.8	9.683	14.96	1.040	1.106	1.075	1.154
	1	9.683	14.96	1.014	1.064	1.020	1.092
bending moment at the bottom of tower (10^3kN/m)	0.2	533.6	1040	1.149	1.135	1.139	0.988
	0.4	533.6	1040	1.052	1.174	1.091	1.113
	0.6	533.6	1040	0.983	1.188	1.006	1.176
	0.8	533.6	1040	0.936	1.088	0.954	1.157
	1	533.6	1040	0.911	1.025	0.921	1.050
damping coefficient		5000		7000		10000	
		ordinary	long	ordinary	ordinary	long	ordinary
velocity index		normalized value		normalized value		normalized value	
shear forces at the bottom of tower	0.2	1.211	2.125	1.325	2.208	1.466	2.172
	0.4	1.111	1.280	1.134	1.362	1.206	1.571
	0.6	1.107	1.644	1.116	1.291	1.130	1.204
	0.8	1.086	1.224	1.105	1.324	1.114	1.261
	1.0	1.032	1.136	1.043	1.166	1.059	1.191
bending moment at the bottom of tower	0.2	1.514	1.495	1.604	1.504	1.734	1.699
	0.4	1.136	1.000	1.212	1.111	1.374	1.392
	0.6	1.070	1.119	1.121	0.980	1.179	1.048
	0.8	0.989	1.159	1.016	1.142	1.060	1.089
	1.0	0.940	1.098	0.957	1.124	0.979	1.137

* 'ordinary' stands for ordinary period seismic wave, 'long' stands for long-period seismic wave.

As Table 4 shows, internal force under long period ground motion is larger than that of ordinary seismic waves, the shear force at the bottom of tower increases by 54.5%, and the bending moment increases 94.9%. When the velocity index is less than or equal to 0.4, the force response under both ordinary and long period ground motion are negative. In addition, except α =0.6 and C =5000, the normalized ratio of internal force is between 0.911~1.324 in other situation which can be considered to that the stress state is in acceptable range.

Discussion of reasonable parameters

In conclusion, in order to decrease the impact on the long-span cable-stayed bridge under different period ground motion, combined with analysis of displacement and internal force, the viscous dampers are setting with reasonable parameters is beneficial to the seismic response controlling of the structure. The displacements of key nodes can be reduced effectively by the nonlinear viscous dampers, and the stress state of structure is improved. Whether the structural displacement response or the internal force response, the long period seismic motion is more unfavourable than the ordinary periodic seismic motion. When the viscous damper parameter is chosen, the damping effect of long period ground motion should be taken as the main role. According to the analysis of Erdong Yangtze River Bridge, for the long-span cable-stayed bridge

under the long period seismic wave, the reasonable parameter of nonlinear viscous dampers is that velocity index α=0.6, damping coefficient C=7000 $N \cdot (s/m)^{\alpha}$.

CONCLUSION

As Erdong Yangtze River Bridge for the engineering background, seismic responses of long-span cable-stayed bridge with and without nonlinear viscous dampers under different period seismic waves are analysed. The characteristics of ground motion in time domain and frequency domain are considered, and the viscous dampers are simulated by Maxwell model. The velocity index and damping coefficient of damper are analysed, and the conclusions and future work are summarized as followed:

(1) Compared with the ordinary period seismic waves, long-period seismic waves have abundant long period components, and are long duration. The peak acceleration of them are generally small, and frequency are concentrated in the low frequency band. Also, the amplification coefficient β of long period seismic waves in long period part is larger than that of ordinary seismic wave.

(2) The displacement and internal force responses of long-span cable-stayed bridge under long period seismic wave are more negative. The seismic design which includs choosing the parameters of viscous dampers should be taken the damping effect of long-period ground motion in the main role.

(3) The nonlinear viscous dampers can effectively reduce the displacement of key nodes of long-span cable-stayed bridges under long period ground motion. The longitudinal relative displacement at the top of the tower and the longitudinal displacement at the beam end are reduced by 60.2% and 46.9% respectively in maximum reduction range. The seismic displacement response is significantly improved.

(4) The combination of velocity index and damping coefficient of nonlinear viscous damper has great influence on the internal force response of long-span cable-stayed bridges. Some parameters will lead to that the shear force and bending moment at the bottom of tower increases sharply and have adverse effects on the structure; but the reasonable parameter combination can control the growth amplitude of the shear force in the acceptable range, and ensure that the bending moment at the bottom of the tower has no obvious increase phenomenon.

(5) Under the action of long period ground motion, combined with displacement and internal force response analysis, the ideal parameters of viscous dampers are that the velocity index α=0.6 and damping coefficient C=7000 $N \cdot (s/m)^{\alpha}$.

(6) In the future work, the numerical parameter fitting method can be used to obtain the optimal results within the limited data.

ACKNOWLEDGEMENTS

This work was supported by National Natural Science Foundation of China (Grant No: 51408449) and the Fundamental Research Funds for the Central Universities (Grant No: 125206004).

REFERENCES

[1] Kim T.H., Lee K.M., Chung Y.S., et al, 2005. Seismic Damage Assessment of Reinforced Concrete

Bridge Columns. Engineering Structures, vol. 27: 576-592.
[2] Hwang J.S., Hung C.F., Huang Y.N., et al, 2010. Design Force Transmitted by Isolation System Composed of Lead-rubber Bearings and Viscous dampers. International Journal of Structural Stability & Dynamics, vol. 10: 287-298.
[3] Geng F., Ding Y., Li A., 2016. Passive Control System for Mitigation of Longitudinal Buffeting Responses of a Six-Tower Cable-Stayed Bridge. Mathematical Problems in Engineering, vol. 1: 1-18.
[4] Wu B.X., Wang L., Wang Z.F., 2007. A Method of Seismic Response Analysis for Bridge with Nonlinear Viscous Damper. Journal of Highway and Tramsportation Research and Development, vol. 24: 76-80.
[5] Xue Y.T., Han X., 2005. Time-history Analysis of Earthquake Response on Structure with Non-linear Fluid Viscous Damper. Earthquake Resistant Engineering and Retrofitting, vol. 27: 40-45.
[6] Terenzi G., 1999. Dynamics of SDOF Systems with Nonlinear Viscous Damping. Journal of Engineering Mechanics, vol. 125: 956-963.
[7] Fournier J.A., Cheng S.,2014. Impact of Damper Stiffness and Damper Support Stiffness on the Efficiency of a Linear Viscous Damper in Controlling Stay Cable Vibrations. Journal of Bridge Engineering, vol. 19: 04013022.
[8] Zhu J., Zhang W., Zheng K.F., et al, 2016. Seismic Design of a Long-Span Cable-Stayed Bridge with Fluid Viscous Dampers. Practice Periodical on Structural Design & Construction, vol. 21: 04015006.
[9] Wu S.P., Zhang C., Fang Z.Z., 2014. Design Schemes and Parameter Regression Analysis of Viscous Dampers for Cable-Stayed Bridge. Bridge Construction, vol. 44: 21-26.
[10] Wang B., Ma C.F., Liu P.F., et al, 2016. Parameter Optimization of Viscous Damper for Cable-Stayed Bridge Based on Stochastic Seismic Responses. Bridge Construction, vol. 46: 17-22.
[11] Zhang X.W., Huang J., Wang J.J., 2015. Effect of Cable-Stayed Bridge's Relative Height of Deck on Viscous Damper's Seismic Reduction Behavior. Journal of Vibration and Shock, vol. 34: 43-47.
[12] Maeda T., Iwaki A., Morikawa N., et al, 2016. Seismic-Hazard Analysis of Long-Period Ground Motion of Megathrust Earthquakes in the Nankai Trough Based on 3D Finite-Difference Simulation. Seismological Research Letters, vol. 87: 1265-1273.
[13] Shoji, G., Kitahara, J., Kojima, A., et al, 2008. Mechanism of seismic response of a pc cable-stayed bridge subjected to a long-period seismic excitation. Journal of Jsce, vol. 25: 91-110.
[14] Barone G., Navarra G., Pirrotta A., 2008. Probabilistic response of linear structures equipped with nonlinear damper devices (PIS method). Probabilistic Engineering Mechanics, vol. 23: 125-133.
[15] Wang Z.Q., Hu S.D., Fan L.C.,2005. Research on Viscous Damper Parameters of Donghai Bridge. China Journal of Highway and Transport, vol. 18: 37-42.
[16] Wang X.R., Shen Y.J., Yang S.P., 2016. A Comparison Study on Kelvin and Maxwell Model for a Forced Single Degree-of-freedom System. Joural of Shijiazhuang Tiedao University (Natural Science Edition) , vol. 29: 70-75.